ELECTRON PARAMAGNETIC RESONANCE IN $RbH_3(SeO_3)_2:Cr^{3+}$ CRYSTALS

By S. Jerzak, S. Waplak

Institute of Molecular Physics, Polish Academy of Sciences, Poznań*

L. A. Shuvalov and R. M. Fedosyuk

Institute of Crystallography, USSR Academy of Sciences, Moscow**

(Received April 8, 1980; final version received June 17, 1980)

Coordination and spin Hamiltonian parameters have been examined for two types of paramagnetic Cr^{3+} centres in $RbH_3(SeO_3)_2$ monocrystal. On the basis of temperature analysis of the EPR spectrum in the range (77–300)K a different type of coupling between the complexes I and II and the lattice has been found. Due to the new method EMM EPR was possible to examine the superstructure occurring below the T_c as a result of the symmetry change $P2_12_12_1$ to $P2_1$ and to define the relation between the splitting of the EPR spectrum and the domain structure. The η order parameter determined from EPR measurement corresponds to the rotation of the SeO_3 groups in the ferroelectric phase.

PACS numbers: 61.16.Hn, 77.80.Bh, 76.30.−v

1. Introduction

The discovery, in 1969, of the ferroelectric properties of rubidium trihydrogen selenite crystal $RbH_3(SeO_3)_2$ is due to Shuvalov and his co-workers [1]. RHS, as shown in Ref. [3] belongs to the group of improper ferroelectrics. Its thermal, elastic, ferroelectric and other properties have since been dealt with in number of papers [2–10]. Of especial interest is the isotopic effect in RHS crystal. In Ref. [11] increasing deuteration is shown to cause a stronger and stronger decrease in spontaneous polarization. In the completely dueterized

* Address: Instytut Fizyki Molekularnej PAN, Smoluchowskiego 17/19, 60–179 Poznań, Poland.
** Address: Institute of Crystallography, Academy of Sciences, 117333 Moscow, USSR.

crystal the phase transition is retained and occurs at practically the same temperature [3].

It is thus important to elucidate the phase transition mechanism of these uncommonly interesting crystals.

The following selenites have hitherto been studied in our Laboratory by Cr^{3+} ion EPR: $NaH_3(SeO_3)_2$ [12, 13] and $KH_3(SeO_3)_2$ [14]. Information concerning the dynamics of the structure near the phase transition can be obtained both by EPR and NMR.

NMR studies of the protons of RHS have been carried out by Silvidi and co-workers [15]. Tokoshima [16] studied NMR on ^{87}Rb in $RbD_3(SeO_3)_2$. EPR studied of γ-irradiated RHS have been performed by Sergeyev et al. [17].

The present work is aimed at determining coordination of Cr^{3+} in RHS and the dynamics of its EPR spectrum in the phase transition region.

2. The crystallographical structure of RHS

The crystallographical structure of RHS crystal at room temperature has been studied by two research groups working independently [18, 19, 21]. The unit cell of RHS has been found to contain 4 molecules, with one Rb^+ cation and two polar SeO_3^{-2} groups constituting an independend element of the structure. The Se—O distance exhibit strong dispersion but are similar within the groups $(SeO_3)_I$ and $(SeO_3)_{II}$. The groups of type I are bonded by hydrogen bridges O_2—H—O_3 = 2.50 Å to form zigzag-like chains along the crystallographical *c*-axis. Another hydrogen bridge O_4—H—O_6 = 2.62 Å bonds $(SeO_3)_{II}$ groups into similar chains disposed along *b*-axis. A third bridge O_1—H—O_5 = 2.53 Å bonds the chains of the types I and II to one another.

The crystallographical inequivalence of the groups $(SeO_3)_I$ and $(SeO_3)_{II}$ is apparent in this disposition with respect to the Rb^+ ion. The octahedron surrounding the latter is composed of 3 oxygens of $(SeO_3)_I$ groups and 5 oxygens of $(SeO_3)_{II}$ groups. The Rb^+ ion is more strongly bonded to the $(SeO_3)_{II}$ than to the $(SeO_3)_I$ groups. At T_c = 153 K RHS undergoes a phase transition with a change in symmetry from $P2_12_12_1$ to $P2_1$, with doubling in magnitude of unit cell along the *c*-axis, and the emergence of spontaneous polarization along the *b*-axis. X-ray [20–22] and EPR results confirm that.

Neutrographical studies of the RHS structure at low temperature (below T_c) by Grimm and Fitzgerald [20] have shown the ordering parameter of the transition to be related with rigid rotations of SeO_3 tetrahedra belonging to chains of a given type, but Grimm did not explain the mechanism which causes the appearance of the spontaneous polarization.

3. Experimental

A. Anisotropy of the EPR spectrum. Parameters of the spin Hamiltonian

The anisotropy of EPR spectrum of Cr^{3+} in RHS was studied at 9.4 GHz in coordinates *XYZ*, where $X = b$ (6.24 Å); $Y = a$ (17.90 Å); $Z = c$ (5.89 Å) in conformity with the system of crystallographical axes proposed by Tovbis et al. [18].

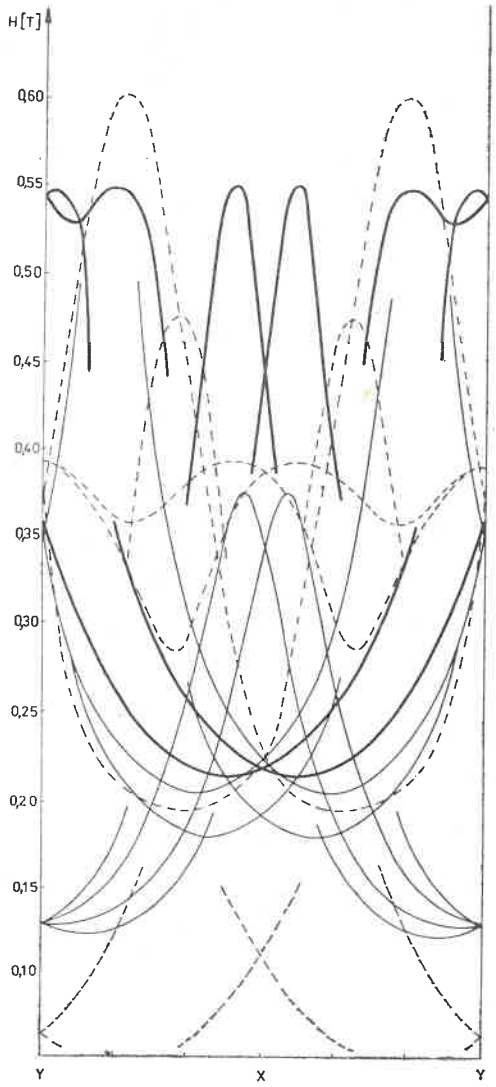

Fig. 1. EPR spectrum anisotropy in the crystallographical *XY*-plane. Continuous thick line — complex I; continuous thin line — complexes II and II′; dashed line — complex III

Fig. 1 shows the above anisotropy in the *XY*-plane. The paramagnetic complexes of the Cr^{3+} ion fall in 4 groups: I, II, II′, III. Those of group I yield the greatest intensity.

The complexes II′ go over to the complexes II as the temperature decreases. The complex III is the weakest; its anisotropy taken at 170 K, is plotted as a dashed line. It was not studied more closely.

Table I gives the directional cosines for the inequivalent complex I, II, and II′.

The EPR lines originating from complex I have a width several times greater than lines of complex II. The I/II intensity ratio differs from one crystal to another. The spectrum

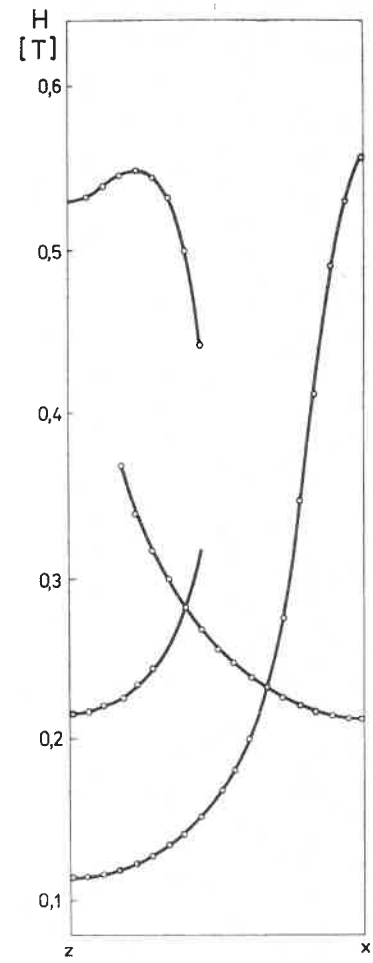

Fig. 2

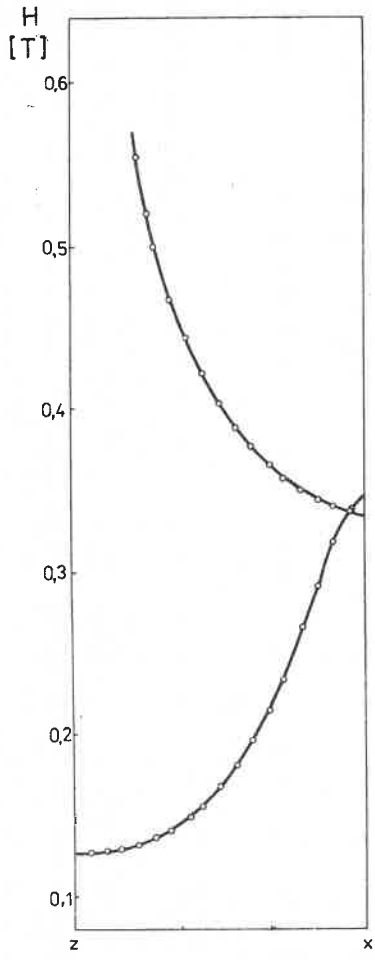

Fig. 3

Fig. 2. Anisotropy of complex I in the principal XZ-plane. Continuous line — theoretical curve; little circles — experimental values

Fig. 3. Anisotropy of complex II in the principal XZ-plane. Continuous line — theoretical curve; little circles — experimental values

of all the complexes is expressed by a spin Hamiltonian of the form:

$$\mathscr{H} = g\beta \boldsymbol{H} \cdot \boldsymbol{S} + D[S_z^2 - \tfrac{1}{3} S(S+1)] + E(S_x^2 - S_y^2). \tag{1}$$

The spin Hamiltonian parameters of complexes I and II calculated with an "Odra 1305" computer, are listed in Table II. Fig. 2 shows the anisotropy of complex (one) I in the principal ZX-plane calculated by computer. The anisotropy, calculated likewise for complex II in the ZX-plane, is shown in Fig. 3. The experimental points plotted in the calculated anisotropy graphs point to a good fit of the spin Hamiltonian parameters.

TABLE I

Direction cosines

	I	II	II′
cos (*x*, *X*)	0.9730	0.8346	0.7458
cos (*x*, *Y*)	−0.2068	−0.1774	−0.2280
cos (*x*, *Z*)	0.1022	0.5215	0.6258
cos (*y*, *X*)	0.0985	0.2059	0.2917
cos (*y*, *Y*)	0.0266	0.9690	0.9542
cos (*y*, *Z*)	−0.9945	0.1361	0.0667
cos (*z*, *X*)	0.2079	−0.5104	−0.5975
cos (*z*, *Y*)	0.9780	0.1722	0.1930
cos (*z*, *Z*)	0.0171	0.8427	0.7765

TABLE II

Parameters of the spin-Hamiltonian

	g	*D* [cm^{-1}]	*a* = *E*/*D*
I	1.980	0.349	0.10
II	1.970	0.540	0.328

B. Study of the spectrum vs temperature

Temperature-dependence studies of the spectrum in the interval (300–77) K shows a different type of temperature-dependence for complex II compared to that of complex I. In the interval (293–170) K an activation process of exchange in intensities takes place between the EPR lines of complexes II′ and II. Fig. 4 shows the $J_{II}/J_{II'}$ intensity ratio vs

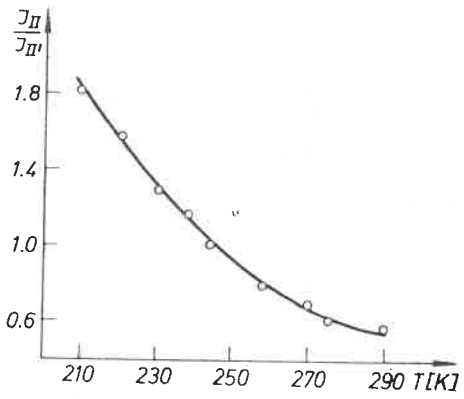

Fig. 4. Intensity ratio of complexes II and II′ vs temperature

temperature; it is well described by the expression:

$$\frac{J_{II}}{J_{II'}} = \exp\frac{\Delta V}{kT}. \tag{2}$$

The graph of ln II/II′ vs the inverse temperature is shown in Fig. 5. The activated energy hence determined for the process in the question amount to $\Delta V = 0.078$ eV.

The EPR lines of complexes II split into 4 components at the ferroelectric phase transition temperature $T_c = 151$ K (Fig. 6). This is in connection with the doubling of the

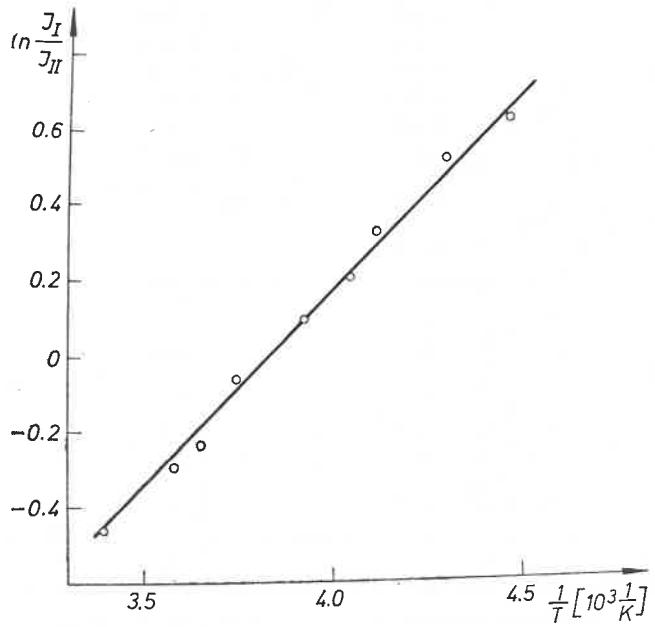

Fig. 5. Graph of ln $I_{II}/I_{II'}$ vs inverse temperature

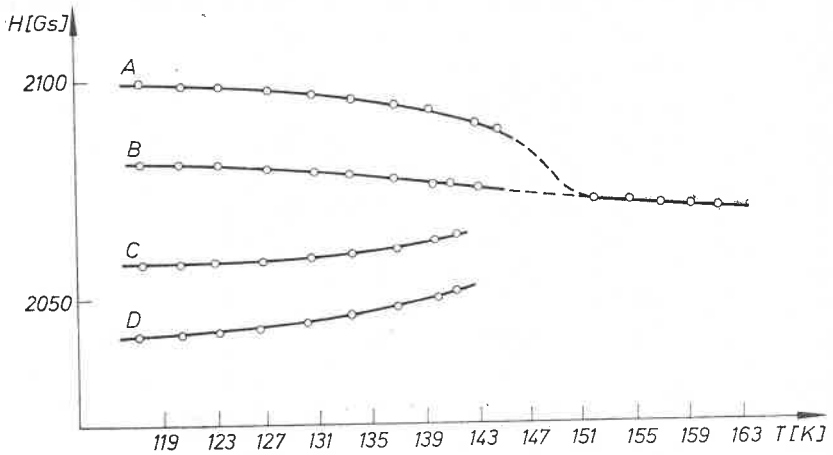

Fig. 6. Splitting of the line $\pm\frac{3}{2} \leftrightarrow \pm\frac{1}{2}$ for complex II in the XY-plane vs temperature

unit cell due to the lowering in symmetry from $P2_12_12_1$ to $P2_1$ and the emergence of the domain structure along the ferroelectric *b*-axis.

The situation is hence similar to that of Cr^{3+} in ARS, studied by Sato [23].

The measuring method EMM EPR, worked out in our Laboratory by Stankowski and Waplak [24], enables us to determine with ease which of the split EPR lines are due to doubling of the unit cell and which to the domain structure. EMM EPR resides essen-

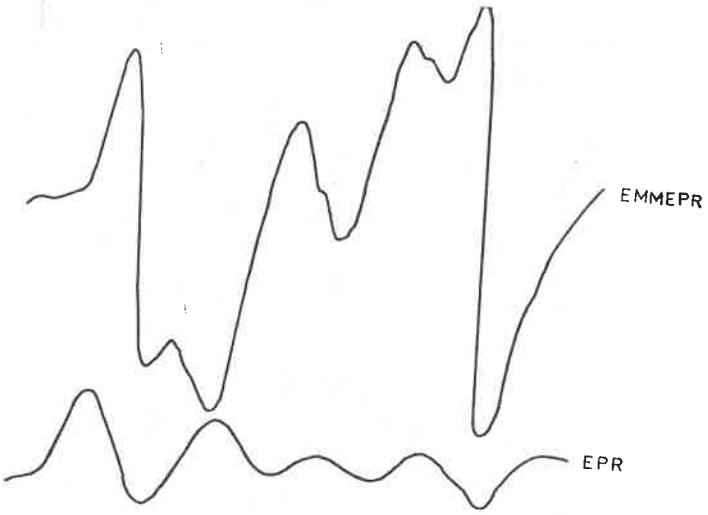

Fig. 7. Magneto-electric modulation (EMEPR) of the four components of the split line of complex II

tially in simultaneous modulation of the magnetic field, in the EPR resonator (classical double EPR modulation) and modulation with an 80 Hz AC field, supplied directly to the electrodes on the ferroelectric and synchronus detection of the signal from the series connected 100 kHz and 80 kHz amplifiers. This results of EPR lines from paramagnetic complexes in opposite domains being recorded in opposite phases.

The RHS order parameter expresses the atomic displacement due to phonon instability on the zone boundary which, in this case, is twice degenerate [25]. The relate wave vectors can be represented by the order parameters η_1 and η_2. This instability causes doubling of the unit cell along the *c*-axis and the emergence of super structure in the low temperature phase. Additionally, two domains should appear, corresponding to condensation of one of the value η_1 or η_2.

The reflexes from super-structure in RHS have been measured by the neutron diffraction method [26]. Fig. 7 shows the results obtained by the EMM EPR method which was applied for the EPR lines of Cr^{3+} in the ferroelectric phase. It is obvious from Fig. 7 that EPR, perfected by the use of EMM EPR, permits an easy distinction between the domain structure and the super-structure in improper ferroelectrics. In our feeling the present method is better adapted to the elucidation of structure and super structure in this class of ferroelectrics than the method of neutron diffraction [26].

A great advantage of using EPR of Cr^{3+} in RHS is a possibility of determining the temperature changes of the order parameter η. This parameter can be determined directly from temperature changes of line splitting and intensity in the ferroelectric phase. Fig. 8 shows qualitative variations in splitting of the line $\pm 1/2 \leftrightarrow \pm 3/2$ for complex II. A detail analysis of the parameter temperature changes will be presented in our next paper.

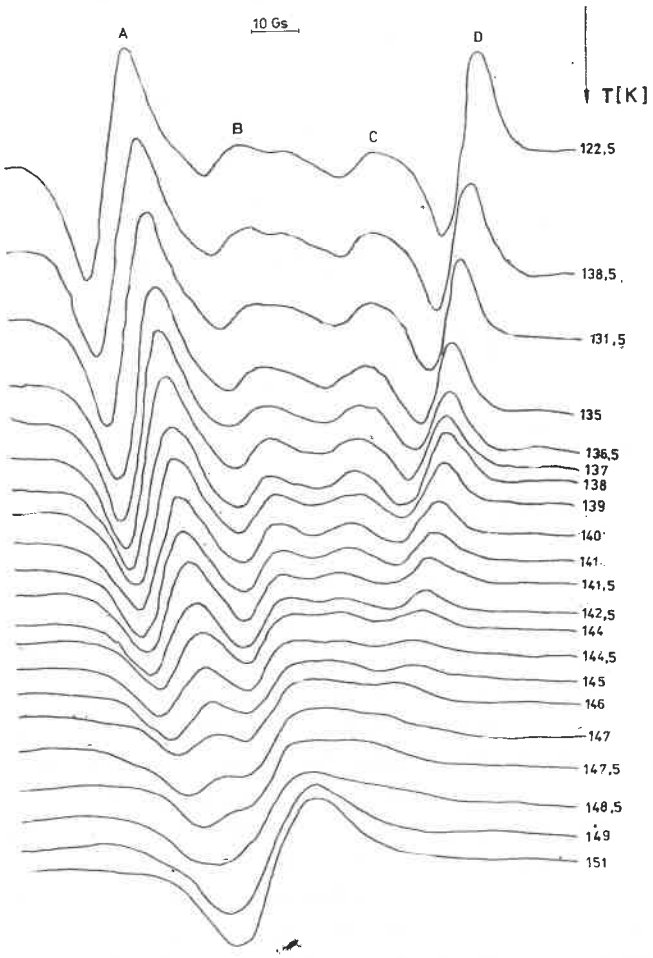

Fig. 8. Temperature variations in splitting of the line $\pm\frac{3}{2} \leftrightarrow \pm\frac{1}{2}$ for complex II. (The low intensity of the central lines shows the crystal to be an almost one-domain one)

The EPR line splitting of the complex II apparent below T_c in the principal direction of the complex is of the structural type and can be described on the bases of changes in the parameter $a = E/D$, which is proportional to the rotation angle $\Delta\varphi$ of the principal axis of complex II. A change of the angles $\Delta\varphi$ corresponds to a change of the order parameter η (Fig. 9). Fig. 10 shows a shift of minima of four splitted EPR lines (two of them rise due to the doubling of the unit cell) when crystal is rotated along b-axis.

It should be noted that the lines associated with Cr^{3+} ions occuring in domains characterized by opposite oriented polarization, reach the minimum values of the H magnetic field for the same φ angle. The lines which originated due to the doubling of unit cell achieve this minimum values of the H field for angels differing by 4.5° at temperature 115 K. It is probably connected with the rotation of the SeO_3 groups around the Y-axis in ferroelectric phase since in XY and YZ planes the splitted lines reach extreme values of H

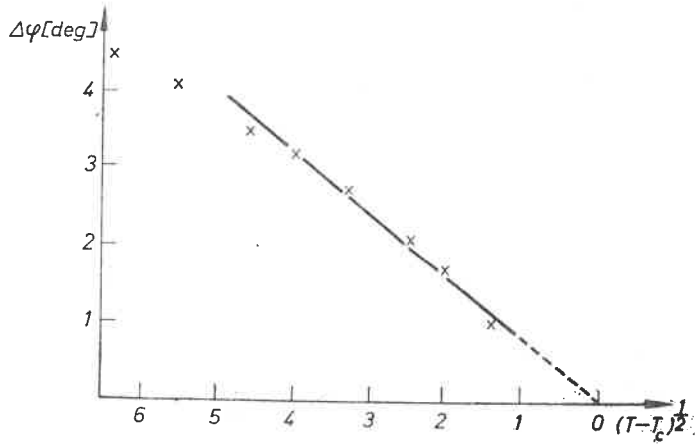

Fig. 9. Change of the rigid rotation angle $\Delta\varphi$ of the $(SeO_3)_{II}$ groups, wich is the order parameter η, vs $(T-T_c)^{\frac{1}{2}}$

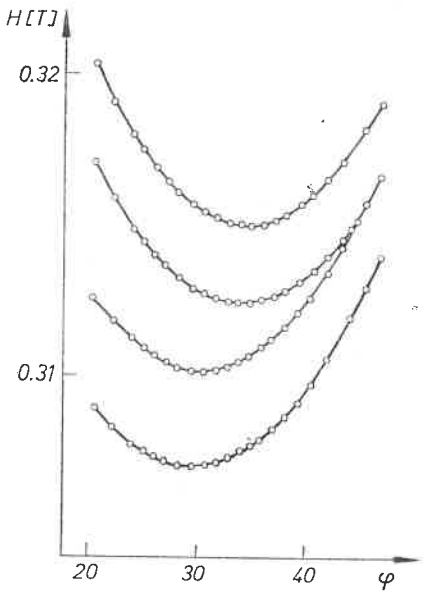

Fig. 10. Anisotropy of the four splitted EPR lines below T_c (115 K) in XZ-plane. The rotation angle $\Delta\varphi$ is measured from the Z-axis

field at the same angle. The angle is smaller than the angle value found by Grimm and Fitzgerald [20], but it should be taken into account that only three of eight oxygens surrounding the Cr^{3+} ion derive from the SeO_3 groups rotating in ferroelectric phase. As the temperature is lowered, both the width and position of $\pm 3/2 \leftrightarrow \pm 1/2$ lines of complex I

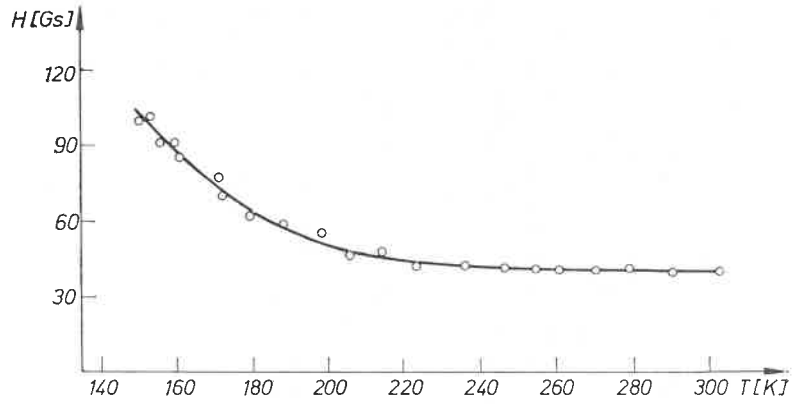

Fig. 11. Width of the line $\pm\frac{3}{2} \leftrightarrow \pm\frac{1}{2}$ vs temperature, for complex I

undergo a change. Below 140 K the EPR spectrum of complex I permits the determination of activation energy of the process from the relation leading to a value of 0.037 eV.

$$\Delta H_T = \Delta H_c \exp \frac{-\Delta V}{kT} . \tag{3}$$

The changes in EPR linewidth vs. temperature for complex I are plotted in Fig. 11.

4. Model of the paramagnetic Cr^{3+} ion centre in RHS

The Rb^+ ion in RHS single crystal is surrounded by oxygens of SeO_3 groups. From the analysis of the EPR spectrum anisotropy for the crystal, we pressume Cr^{3+} to occupy the site of an Rb^+ ion. The introduction of an ion of higher valency into the RHS lattice requires compensation by two Rb^+ vacancies, as in the case of $NaH_3(SeO_3)_2$ [12, 13] and $KH_3(SeO_3)_2$ [14]. The excess charge can be compensated by two Rb^+ vacancies or two protonic vacancies.

On the basis of the NMR work of Silvidi et al. [15] on RHS, two relaxation times T_1 and T_1' were found for the protons. T_1 differs from T_1' by one order of magnitude. The difference in temperature dependence of the EPR spectra of the Cr^{3+} complexes I and II point to the presence of two distinct proton vacancies compensating the exess charge of the Cr^{3+} in RHS. The protons compensating complex I are at greater distance from the Cr^{3+} ion than in the case of complex II. This auggests a lower value of D, the trigonal component of which is proportional to $1/R^3$ where R is the distance between Cr^{3+} and the protonic vacancy. The EPR linewidth seen in Fig. 10 is related with fluctuations of the

fine structure parameter D. The activation energy determined for this process amounts to $\Delta V = 0.037$ eV. Complex II is compensated by way of protonic vacansies, which undergo disruption and ordering below T_c.

Proton ordering and the rotational motion of $(SeO_3)^{-2}$ groups related hitherto occurs at lower temperatures than translational motions, which are presumbly related with an earlier disruption of the weaker hydrogen bonds.

5. Discussion of the results

Structurally, the various selenite monocrystals differ most strongly by their spatial configurations of hydrogen bonds. The structures have in common an elementary zigzag chain of hydrogen-bonded SeO_3 groups. In $NaH_3(SeO_3)_2$, the elementary chains are bonded so as to form a planar lattice; in $RbH_3(SeO_3)_2$, two systems of mutually perpendicular hydrogen bonds are additionally connected by a hydrogen bridge so as to form three-dimensional carcasse [18]. Available results concerning the spin-lattice relaxation times for the protons as well as our results relating to the temperature-dependent behaviour of the complexes of type I and II prove that the hadrogen bonds of RHS are by no means equivalent.

The splitting of the EPR spectrum of Cr^{3+} below T_c is related with rigid rotation of SeO_3 groups, as corroborated by structural studies [20] as well as by the proton ordering due to the roration.

Most probably, already above T_c, the vibration frequency of protons in hydrogen bridges becomes slower in the weaker bridges leading to modulation of the parameter D of complex I, compensated by protonic vacancies of this type.

The authors wish to thank Professor Dr habil. J. Stankowski for his interest and discussions troughout the present investigation.

REFERENCES

[1] L. A. Shuvalov, N. R. Ivanov, N. W. Gordeyeva, I. F. Kirpichnikova, *Kristallografiya* **14**, 658 (1969).
[2] N. R. Ivanov, Y. T. Verovskaja, *Izv. Akad. Nauk* **31**, 2563 (1970).
[3] L. A. Shuvalov, N. R. Ivanov, A. M. Shirokov, A. A. Boiko, I. F. Kirpichnikova, N. V. Gordeyeva, A. M. Baranova, A. Fouskova, V. S. Ryabkin, V. A. Babayants, S. H. Akanzarov, *Kristallografiya* **20**, 335 (1975).
[4] V. V. Gladkii, V. K. Magataev, I. S. Zheludev, *Ferroelectrics* **13**, 343 (1976).
[5] V. K. Magataev, V. V. Gladkii, *Fiz. Tverd. Tela* **19**, 583 (1977).
[6] V. V. Gladkii, V. A. Kirikov, V. K. Magataev, L. A. Shuvalov, *Fiz. Tverd. Tela* **19**, 291 (1977).
[7] L. M. Rabkin, V. P. Dimitriev, V. I. Torgashev, L. A. Shuvalov, N. M. Shagina, *Ferroelectrics* **14**, 627 (1976).
[8] H. Poilet, J. P. Mathieu, *Ferroelectrics* **19**, 155 1978.
[9] V. P. Dimitriev, L. M. Rabkin, V. I. Torgashev, L. A. Shuvalov, N. V. Gordeyeva, *Kristallografiya* **22**, 329 (1977).
[10] V. V. Gladkii, L. A. Shuvalov, *Fiz. Tverd. Tela* **20**, 3117 (1978).
[11] V. V. Gladkii, V. K. Magataev, L. A. Shuvalov, R. M. Fedosyuk, *Phys. Lett.* **59A**, 391 (1976).
[12] S. Waplak, A. Małecka, J. Stankowski, *Acta Phys. Pol.* **A47**, 809 (1975).

[13] A. Małecka, J. Stankowski, L. A. Shuvalov, *Ferroelectrics* **15**, 1 (1977).
[14] W. Zapart, S. Waplak, J. Stankowski, L. A. Shuvalov, *J. Phys. Soc. Jpn.* **44**, 1600 (1978).
[15] A. A. Silvidi, D. T. Workman, *Ferroelectrics* **6**, 183 (1974).
[16] T. Takoshima, M. Kasahara, I. Tatsuzaki, *J. Phys. Soc. Ipn.* **46**, 1804 (1979).
[17] N. A. Sergeyev, O. V. Faleev, *Izv. Akad.. Nauk USSR, Ser. Fiz.* **39**, 714 (1975).
[18] A. B. Tovbis, T. S. Davydova, V. I. Simonov, *Kristallografiya* **20**, 103 (1972).
[19] R. Tellegren, R. Liminga, *Ferroelectrics* **15**, 15 (1977).
[20] M. Grimm, W. J. Fitzgerald, *Acta Crystallogr.* **A34**, 268 (1978).
[21] Y. Makita, S. Suzuki, *J. Phys. Soc. Jpn.* **36**, 1215 (1974).
[22] S. Kh. Akanzarov, V. Sh. Shekhtman, L. A. Shuvalov, *Kristallografiya* **19**, 95 (1974).
[23] K. Sato, A. Sawada, Y. Tagagi, Y. Iohibashi, *J. Phys. Soc. Jpn.* **36**, 619 (1974).
[24] J. Stankowski, S. Waplak, *Ferroelectrics* **24**, 223 (1980).
[25] A. P. Levanyuk, D. G. Sannikov, *Fiz. Tverd. Tela* **12**, 2997 (1970).
[26] W. J. Fitzgerald, H. Grimm, *Solid State Commun.* **22**, 749 (1977).